Developmental Biology 456 (2019) 17–24

Contents lists available at ScienceDirect

Developmental Biology

journal homepage: www.elsevier.com/locate/developmentalbiology

Decoupling developmental apoptosis and neuroblast proliferation in *Drosophila*

Katherine Harding, Kristin White *

Massachusetts General Hospital, Cutaneous Biology Research Center, Harvard Medical School, Boston, MA, 02129, USA

ARTICLE INFO

Keywords:
Drosophila
Neuroblast
Apoptosis
Quiescence
Stem cells

ABSTRACT

Cell proliferation and cell death are opposing but fundamental aspects of development that must be tightly controlled to ensure proper tissue organization and organismal health. Developmental apoptosis of abdominal neuroblasts in the *Drosophila* ventral nerve cord is controlled by multiple upstream spatial and temporal signals, which have also been implicated in control of cell proliferation. It has therefore remained unclear whether developmental apoptosis is linked to active cell proliferation. Previous investigations into this topic have focused on the effect of cell cycle arrests on exogenous induction of apoptosis, and thus have not addressed whether potential effects of the cell cycle lie with the sensing of damage signals or the execution of apoptosis itself. In this report, we show that developmental apoptosis is not inhibited by cell cycle arrest, and that endogenous cell death occurs independently of cell cycle phase. We also find that ectopic neuroblasts rescued from cell death retain the competency to respond to quiescence cues at the end of embryogenesis. In addition, we observe multiple quiescence types in neuroblasts, and we show that cell death mutant embryos display a specific loss of presumptive G2 quiescent abdominal neuroblasts at the end of embryogenesis. This study demonstrates that upstream control of neuroblast proliferation and apoptosis represent independent mechanisms of regulating stem cell fate, and that execution of apoptosis occurs in a cell cycle-independent manner. Our findings also indicate that a subset of G2Q-fated abdominal neuroblasts are eliminated from the embryo through a non-apoptotic mechanism.

1. Introduction

Proper tissue organization depends on an appropriate balance of cell proliferation and cell death. In the embryo, the vast majority of both stem cell proliferation and cell death occur in the developing nervous system, prompting us to examine the functional connection between the cell cycle and cell death in this tissue.

In the *Drosophila* ventral nerve cord (VNC), the majority of embryonic abdominal neuroblasts undergo apoptosis prior to the end of embryogenesis (Abrams et al., 1993; White et al., 1994). Between embryonic and larval life, the remaining neuroblasts enter a period of quiescence (Truman and Bate, 1988). Re-activation of neuroblasts depends on stimulation by a combination of developmental and environmental signals (Ebens et al., 1993; Chell and Brand, 2010; Sousa-Nunes et al., 2011). Abdominal post-embryonic neuroblasts are eliminated in a second wave of apoptosis during larval development (Bello et al., 2003). In apoptosis-deficient larvae, abdominal post-embryonic neuroblasts continue to proliferate, indicating that developmentally regulated apoptosis in the larval CNS interrupts active neuroblast proliferation (Bello et al., 2003). However, as no study has investigated the effect of cell cycle arrest on the developmental death of abdominal neuroblasts, it remains unclear whether active proliferation is required for apoptosis.

Cell cycle heterogeneity can contribute to the differential sensitivity of tumor cells to chemotherapies (Pawlik and Keyomarsi, 2004; Ryl et al., 2017; Chao et al., 2017), but the focus on DNA-damaging agents in these studies may confound the cellular processes involved in sensing critical damage and initiating cell death. Previous studies in *Drosophila* examining a potential link between the cell cycle and apoptosis have also relied on exogenously-induced cell death, rather than on developmentally-regulated apoptosis (Fan et al., 2010; Hassel et al., 2013; Qi and Calvi, 2016; Cosolo et al., 2019). Endocycling cells in the oocyte have been found to be resistant to genotoxic stress induced by ionizing radiation (IR; (Hassel et al., 2013; Qi and Calvi, 2016), while G2-arrested cells in imaginal discs are protected from cell death induced by activation of the JNK stress response pathway (Cosolo et al., 2019). As these approaches to induce apoptosis depend on stress-sensing pathways

* Corresponding author.
E-mail address: kristin.white@MGH.Harvard.edu (K. White).

https://doi.org/10.1016/j.ydbio.2019.08.004
Received 4 April 2019; Received in revised form 1 August 2019; Accepted 3 August 2019
Available online 4 August 2019

that lie upstream from the induction of cell death, we wondered whether the observed effects of the cell cycle may be related to the integration of stress or damage signals into the cell death pathway, rather than the activation of apoptosis itself.

Induction of neuroblast apoptosis is controlled by a combination of temporal and spatial factors, including the Hox gene *abdominal-A* (*abdA*) (Bello et al., 2003; Arya et al., 2015; Khandelwal et al., 2017). Loss of *abdA* inhibits apoptosis of abdominal neuroblasts, as *abdA* is required for the activation of an intergenic enhancer that controls expression of genes within the cell death locus (Bello et al., 2003; Arya et al., 2015; Khandelwal et al., 2017). In addition to its role in cell death, *abdA* is implicated in spatial regulation of quiescence. Overexpression of *abdA* in the thoracic NB3-3 lineage prolongs its window of proliferation during embryogenesis, phenocopying the normal abdominal NB3-3 behavior (Tsuji et al., 2008). Neuroblast proliferation, like apoptosis, is thus sensitive to upstream spatial control through development.

In this study, we demonstrate that direct manipulation of neuroblast proliferation does not inhibit developmentally regulated apoptosis, and we observe that multiple steps of cell death activation are cell cycle phase-independent. In addition, abdominal neuroblast survival is not specific to the G0 or G2 type of post-embryonic quiescence recently reported by Otsuki and Brand (2018). We also observed a surprising loss of G2, but not G0, quiescence-type abdominal neuroblasts in the absence of apoptosis, indicating that quiescence type is correlated with cell fate decisions other than cell death. To the best of our knowledge, this report is the first to describe non-apoptotic loss of abdominal neuroblasts during embryogenesis.

2. Results and discussion

2.1. Neuroblast apoptosis is not inhibited by cell cycle arrests

To determine whether apoptosis depends on active neuroblast proliferation, we first tested whether the induction of various cell cycle arrests in neuroblasts was sufficient to rescue them from developmental apoptosis. We arrested neuroblasts by over-expressing *dacapo* (*dap*) or by RNAi knockdown *cycE* or *cycA* under control of the *worniu-GAL4* driver (Albertson et al., 2004). This driver is expressed in neuroblasts and their progeny. Over-expression of *dap* and *cycE-RNAi* lead to G1 arrests, while *cycA-RNAi* leads to a G2 arrest (de Nooij et al., 1996; Lane et al., 1996; Qi and Calvi, 2016, Fig. 1A), allowing us to determine whether arrests at various points of the cell cycle have different effects. We assessed abdominal neuroblast survival at embryonic stage 17 by staining embryos for the pan-neuroblast marker Deadpan (Dpn). Neither over-expression of *dap*, nor knockdown of *cycE* or *cycA* increased the number of abdominal neuroblasts at stage 17 compared to control embryos (Fig. 1A–B), indicating that neither G1-nor G2-arrest is sufficient to inhibit developmental apoptosis in this context. We confirmed that the cell cycle arrests reduce the mitotic index of abdominal neuroblasts without affecting neuroblast numbers (Fig. 1C and Fig. S1), and decrease the number of progeny produced by a single neuroblast (NB3-5) when expressed specifically in that neuroblast using the *VAcht(R59E09)-GAL4* driver (Fig. 1D and Fig. S2; Pfeiffer et al., 2010; Lacin and Truman, 2016). Our data therefore show that inhibition of neuroblast proliferation in the embryo does not prevent neuroblast cell death by developmental apoptosis.

We also confirmed that the cell cycle arrests do not induce ectopic apoptosis, as measured by levels of the cleaved effector caspase Dcp1 (cDcp1; Song et al., 1997; Hay and Guo, 2006). Dcp1 activation involves cleavage of its inactive form into two peptides, therefore execution of apoptosis can be monitored by detection of the cleaved form of Dcp1. We did not observe statistically significant differences in the number of cDcp1-positive neuroblasts at stages 14–16 of embryogenesis (Fig. S2B), however *cycE-RNAi* seemed to result in a precocious wave of developmental apoptosis compared to control embryos. When each of the cell cycle arrests were driven in the NB3-5 lineage (a neuroblast that survives embryogenesis in the abdominal segments; Birkholz et al., 2015; Lacin and Truman, 2016; Fig. S4) using *VAcht-GAL4*, we did not observe loss of the Dpn-positive neuroblast (Fig. S2A), indicating that none of the arrests lead to cell death of this neuroblast.

Our finding that neuroblast cell cycle arrests do not inhibit their developmental cell death is in contrast to previous studies examining the effect of cell cycle arrest on exogenously-induced cell death in other tissues (Hassel et al., 2013; Qi and Calvi, 2016; Cosolo et al., 2019). Taking these previous results together with our observations suggests that, while the upstream mechanisms responsible for sensing external stress may be cell cycle-dependent, the downstream execution of apoptosis is cell cycle-independent. Therefore, stress-induced and developmental apoptosis may turn on distinct upstream pathways that lead to activation of the cell death genes.

2.2. Initiation and execution of apoptosis occurs independently of cell cycle phase

While our previous results indicate that manipulation of the cell cycle does not prevent developmental apoptosis, it remained possible that endogenous cell death could occur predominantly within a particular cell cycle phase. We predicted that if cell death occurs in a specific phase of the cell cycle, activation of the apoptosis pathway would be enriched in neuroblasts in that phase. Neuroblast apoptosis is transcriptionally activated by expression of the cell death genes *grim, reaper* and *sickle* (White et al., 1994; Chen et al., 1996; Peterson et al., 2002; Wing et al., 2002; Srinivasula et al., 2002). Our lab has previously characterized an intergenic cell death enhancer that is required for expression of *grim, reaper* and *sickle,* and which is controlled by *abdA* (Tan et al., 2011; Arya et al., 2015). We have previously generated a transcriptional reporter of this enhancer (Enh1-GFP) that is active specifically in doomed neuroblasts, allowing us to observe the induction of apoptosis *in vivo,* upstream of the cell death genes (Tan et al., 2011; Arya et al., 2015).

We first examined expression of Enh1-GFP in neuroblasts within G2/M phase, as assessed by expression of Cyclin B (CycB), to determine if transcriptional activation of the cell death pathway, as reported by Enh1-GFP, occurs primarily in G2/M phase. We found that during embryonic stages 15–16, approximately 25% of abdominal neuroblasts are positive for Enh1-GFP, and ~50% are positive for CycB expression (Fig. 2A left, 2B). Similarly, within the subset of CycB-positive neuroblasts, approximately 25% are Enh1-GFP, and within the subset of Enh1-GFP-positive neuroblasts, ~50% are CycB-positive (Fig. 2A right, 2B). These conserved proportions suggest that there is no enrichment for Enh1-GFP expression in G2/M phase, or vice versa. Furthermore, we compared the observed frequency of double positive Enh1-GFP + CycB + neuroblasts to the calculated expected frequency of double positive cells if Enh1-GFP and CycB expression were independent events. We found that the expected and observed frequencies are indistinguishable (Fig. 2E), indicating that Enh1-GFP activation is independent of CycB expression.

As Enh1-GFP activation is a relatively upstream event in the cell death pathway, we next assessed whether cell cycle phase was related to activation of the effector caspase Dcp1, which is a downstream event in apoptosis (Song et al., 1997; Hay and Guo, 2006). Consistent with our analysis of Enh1-GFP, we found that cDcp1 staining occurs in the same proportion of the whole population of abdominal neuroblasts and the subset of CycB-positive abdominal neuroblasts (Fig. 2C–D). The proportion of CycB-positive abdominal neuroblasts was also indistinguishable between the populations of all abdominal neuroblasts and the cDcp1+ subset (Fig. 2C–D), while the expected and observed frequencies of double positive cDcp1+CycB + neuroblasts are equal (Fig. 2F). In an independent experiment, we tested whether cDcp1 expression was enriched in the CycB-negative population of abdominal neuroblasts, as a proxy for G1/S phase neuroblasts (Fig. S3). Similar to the results with G2/M phase (CycB+) neuroblasts, we determined that cDcp1 is detected with the same frequency in the entire abdominal neuroblast population and the CycB-negative subset, and that the observed frequency of

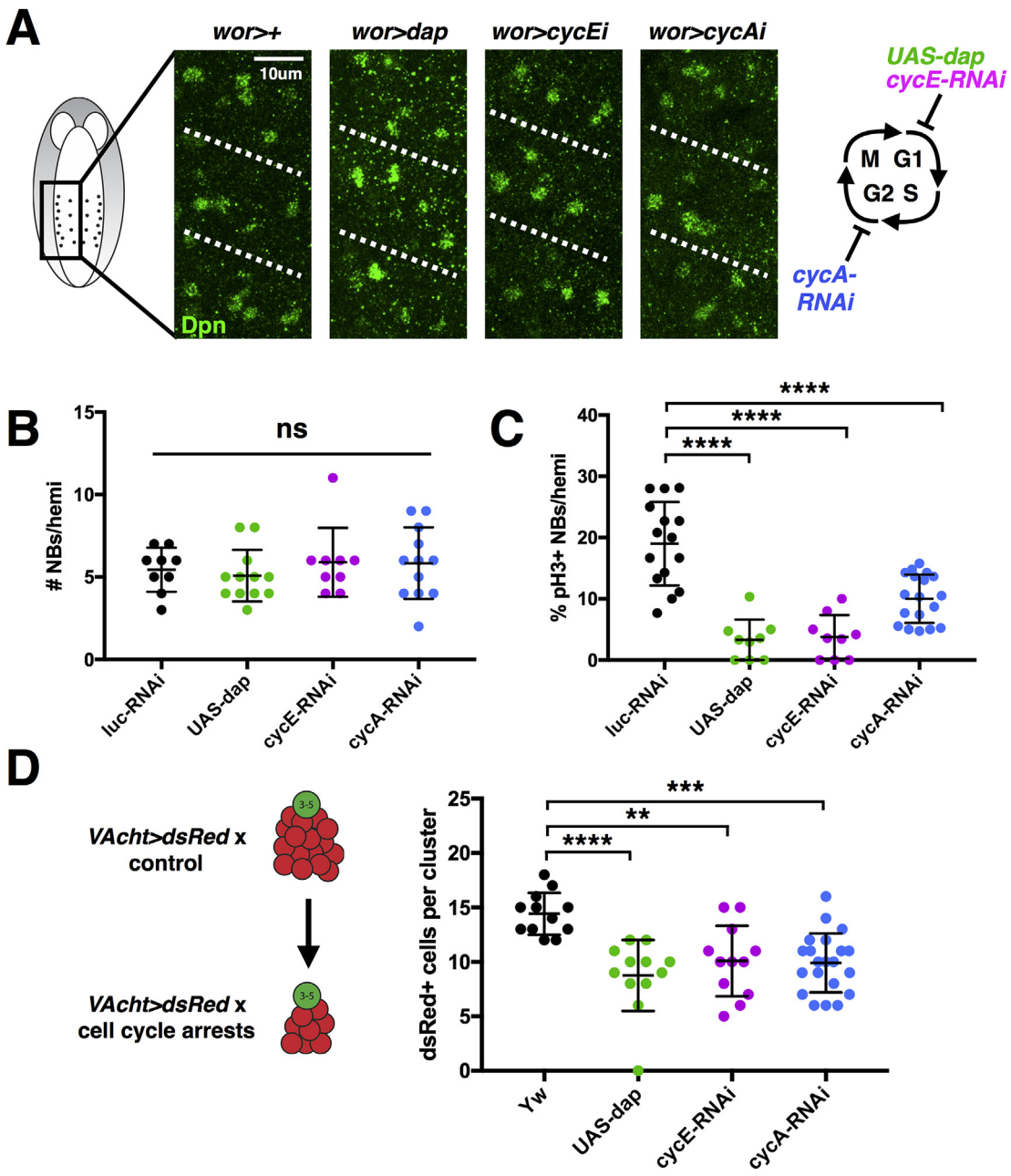

Fig. 1. Cell cycle arrests do not inhibit developmental apoptosis. (A) Induction of ectopic cell cycle arrests in neuroblasts using the *worniu-GAL4* driver does not prevent their cell death at the end of embryogenesis. Embryos were stained with anti-Dpn to visualize neuroblasts and three abdominal hemisegments of stage 17 embryos from each genotype are shown. White dashed bars separate hemisegments of the nervous system. The expected effect of each genotype on the cell cycle is shown on the right. **(B)** The number of neuroblasts per 3 abdominal hemisegments was quantified in a *dcr2; wor-GAL4* background. Data in **B** are individual hemisegment counts from >3 embryos per genotype at stage 17. By this stage the vast majority of neuroblast apoptosis has occurred, but we consistently observe a small number of additional cells per hemisegment in wild type embryos that will be eliminated from the nervous system by larval hatching. **(C)** Ectopic cell cycle arrests in the *dcr2; wor-GAL4* background significantly reduce neuroblast proliferation. Data in **C** are individual hemisegment counts from >3 embryos per genotype at stage 14. **(D)** The ectopic cell cycle arrests also significantly reduce the number of dsRed + progeny produced by NB3-5 when expressed in this lineage using the *VAcht-GAL4* driver. Data in **D** are pooled from >4 embryos (3 clusters each) at stage 17.

cDcp1+CycB- abdominal neuroblasts is equal to the expected frequency if cDcp1 and CycB expression were independent events (Fig. S3). We conclude from these results that both transcriptional activation of the cell death pathway and caspase cleavage events occur independently of cell cycle phase during endogenous developmental apoptosis.

2.3. Post-embryonic neuroblast survival is not specific to quiescence type

Embryonic neuroblasts proliferate throughout development until stage 17, at which time all neuroblasts that remain in the nervous system enter a period of quiescence (with the exception of four mushroom body neuroblasts within the optic lobes) (Truman and Bate, 1988; Ito and Hotta, 1992; Britton and Edgar, 1998). We sought to test whether cell cycle dynamics were consistent between surviving neuroblasts by monitoring nuclear CycB expression levels in abdominal NB3-5 and NB5-3 in embryonic stages 13–17. To visualize surviving neuroblasts *in vivo*, we used two drivers previously characterized by Lacin and Truman, (2016) that are expressed in either NB3-5 alone (*VAcht-GAL4 [R59E09]*),

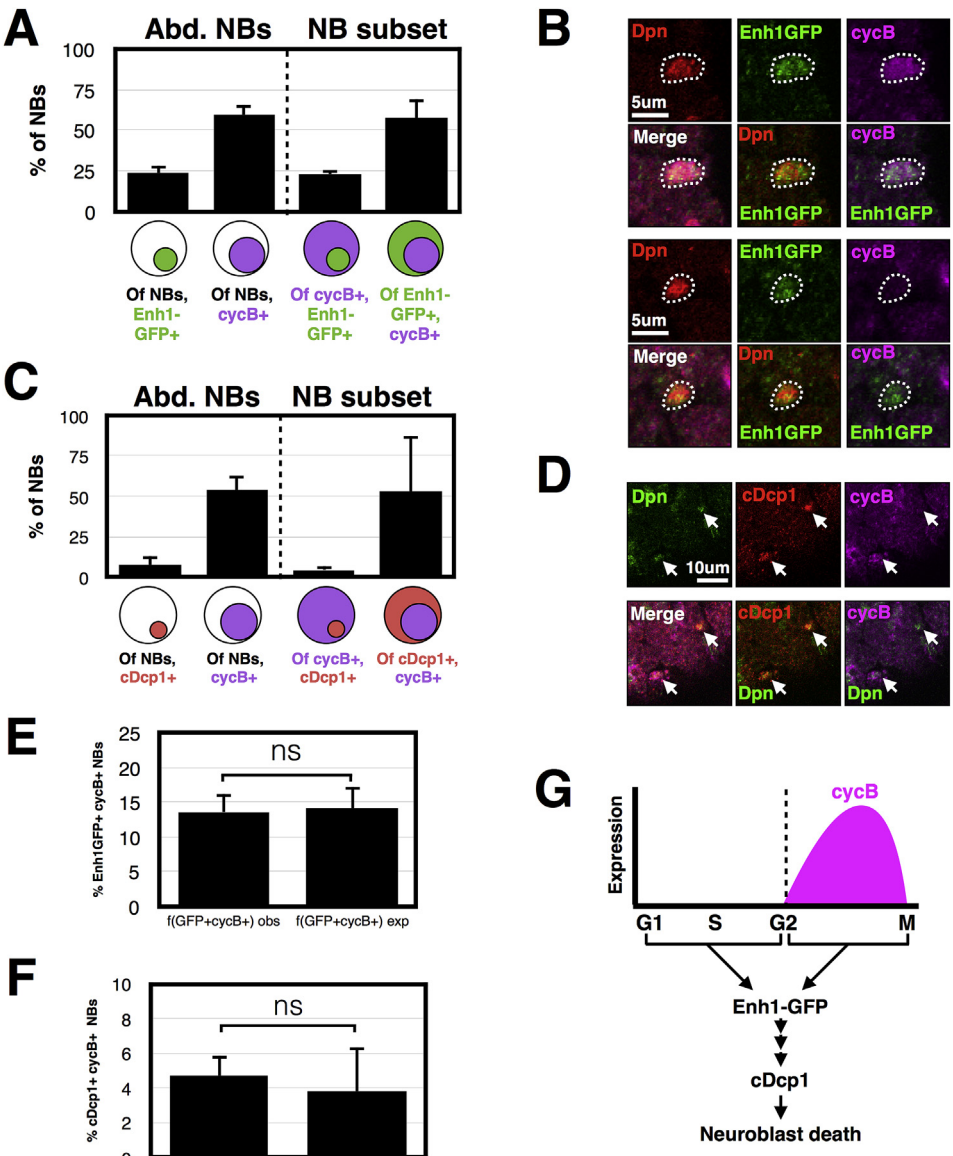

Fig. 2. Apoptosis is initiated and executed independently of cell cycle phase. (A–B) In wild type embryos, there is no enrichment of Enh1-GFP-positive neuroblasts (fated to die) within the CycB-positive subset of neuroblasts (right), compared to the general abdominal neuroblast population at stage 15–16 (left, n = 120 cells from 4 embryos). There are no statistically significant differences between the number of Enh1GFP + or CycB + neuroblasts in the general population compared to the subsets ([% Enh1GFP + all abd. NBs] vs. [% Enh1GFP+ of CycB + abd. NBs]: p-value = 0.733; [% CycB + all abd. NBs] vs. [% CycB+ of Enh1GFP + abd. NBs]: p-value = 0.869). Images shown in **B** are single confocal stacks, and illustrate that Enh1-GFP can be observed in both CycB-positive and -negative neuroblasts (outlined in white dotted lines). **(C–D)** There is also no enrichment of cDcp1-positive neuroblasts (with activated caspase) within the CycB-positive subset of neuroblasts (right), compared to the general population at stage 15–16 (left, n = 287 cells from 8 embryos). There are no statistically significant differences between the number of cDcp1+ or CycB + neuroblasts in the general population compared to the subsets ([% cDcp1+ all abd. NBs] vs [% cDcp1+ of CycB + abd. NBs] p-value = 0.225; [% CycB + all abd. NBs] vs [% CycB+ of cDcp1+ abd. NBs] p-value = 0.962). **D** shows a single confocal section in which cDcp1 staining can be seen in both CycB-positive and -negative neuroblasts (arrows indicate cDcp1+ neuroblasts). **(E–F)** For both Enh1-GFP and cDcp1 with CycB, the observed frequency of double positive neuroblasts is not significantly different from the expected frequency if the expression patterns are independent events. The expected frequency of double positive neuroblasts assuming statistical independence was calculated by multiplying the proportions of single positive neuroblasts in individual embryos; mean and standard deviation of 4 **(E)** and 8 **(F)** embryos are shown. **(G)** Model describing the relationship between neuroblast Cyclin B expression and activation of cell death. CycB protein levels rise during G2/M phases, before dropping precipitously with the onset of anaphase. Activation of both the Enh1GFP cell death reporter and the caspase Dcp1 can occur in CycB-positive and CycB-negative neuroblasts, indicating that apoptosis can be initiated and executed throughout the cell cycle in neuroblasts.

or a subset of neuroblasts including the survivor NB5-3 (*calx-GAL4 [R54D04];* Figs. S4A and B). We confirmed that both drivers are expressed in a single neuroblast per hemisegment at stage 17 (Fig. S4C), indicating that they accurately identify a surviving neuroblast.

Intriguingly, we observed high nuclear expression of CycB in NB3-5 at stage 17, while CycB levels remained low in NB5-3 at this time (Fig. 3). This observation suggested that NB3-5 enters quiescence in G2/M phase, rather than displaying a more canonical G0 quiescence. Our finding is consistent with the report of Otsuki and Brand (2018), who determined that in thoracic segments, NB3-5 arrests in G2 (G2 quiescence; G2Q), while NB5-3 enters a G0 arrest at the end of embryogenesis. Our results confirm that the quiescence patterns of these neuroblasts in the thoracic segments are conserved in the abdominal regions. As the two surviving post-embryonic neuroblasts that we are able to identify *in vivo* display distinct types of quiescence, we conclude that the neuroblast survival fate is not dependent on the upstream mechanisms that distinguish either G0 or G2Q arrests.

2.4. Ectopic neuroblasts are competent to respond to quiescence cues

Finally, we wondered whether the ability to enter into quiescence at the end of embryogenesis was restricted to neuroblasts fated to survive. *abdA* has previously been shown to promote neuroblast proliferation, and it is also necessary for apoptosis of abdominal neuroblasts (Bello et al., 2003; Tsuji et al., 2008; Arya et al., 2015). Given that *abdA* regulates multiple neuroblast cell fate decisions, we wondered whether it also regulates neuroblast entry into quiescence. *abdA-RNAi* knockdown significantly increased the number of abdominal neuroblasts at stage 17 compared to control as expected (Fig. 4A–B). However, the ectopic neuroblasts remained pH3-negative as in wild type (Fig. 4A, C), indicating that they cease proliferating at the end of embryogenesis. To determine whether this result is specific to neuroblasts rescued by loss of *abdA*, we also assessed pH3 staining in neuroblasts rescued by over-expression of the pan-caspase inhibitor p35. We found that ectopic abdominal neuroblasts generated by p35 over-expression also enter

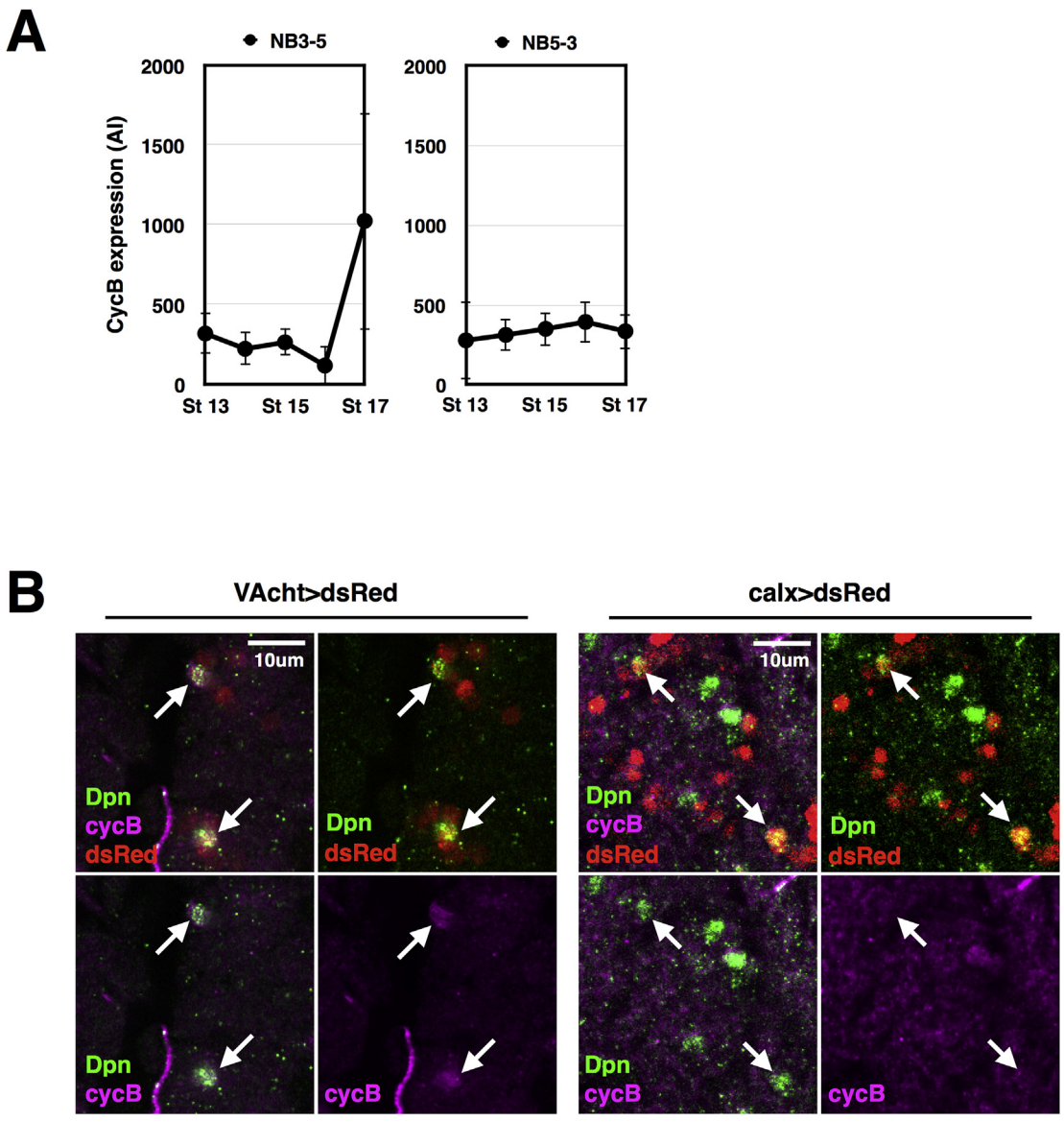

Fig. 3. Post-embryonic neuroblast survival does not correlate with quiescence type. (A–B) Abdominal NB3-5 (identified by *Vacht* > *dsRed*) and NB5-3 (*calx* > *dsRed*), both neuroblasts that will survive to post-embryonic stages, display differential CycB expression at stage 17 (total n > 3 neuroblasts per time-point). Images in **B** are single confocal sections, arrows indicate two abdominal NB3-5 cells (left) and two abdominal NB5-3 cells (right), as determined by co-expression of Dpn and dsRed. While both neuroblasts are quiescent at stage 17, NB3-5 arrests in G2 phase with nuclear CycB and NB5-3 displays a CycB-negative G0 arrest.

quiescence at stage 17 (Fig. 4A–C). These data indicate that ectopic neuroblasts in the abdominal region generated by inhibition of cell death are competent to respond to upstream signals that drive entry into quiescence. Furthermore, this effect is not specific to loss of *abdA*, which has been shown to regulate neuroblast proliferation in other contexts, as neuroblasts rescued by p35 also become quiescent at the end of embryogenesis.

2.5. G2Q-type neuroblasts are lost in the absence of apoptosis

We next wondered whether the G2Q/G0 quiescence patterns described in the thorax are maintained in ectopic abdominal neuroblasts rescued from apoptosis. We first inhibited apoptosis with either *abdA-RNAi* or *UAS-p35*, and quantified the ratio of CycB+ (G2Q) and CycB- (G0) neuroblasts in thoracic and abdominal hemisegments at stage 17 of embryogenesis. Similar to Otsuki and Brand (2018), we observe that the thoracic hemisegments of wild type embryos contain approximately 2.5-fold more G2Q neuroblasts than G0 quiescent neuroblasts (Fig. 4D). In contrast to the thorax, abdominal hemisegments contain a ratio of approximately 1.8 G2Q to G0 neuroblasts, but these hemisegments contain many fewer neuroblasts at the end of embryogenesis compared to the thoracic hemisegments.

When apoptosis was inhibited with *abdA-RNAi* or *UAS-p35*, we observed an increase in the number of abdominal neuroblasts at stage 17 as expected. *abdA-RNAi* and *UAS-p35* significantly increased the number of both CycB+ and CycB- abdominal neuroblasts compared to wild type. However, neither of these genotypes were able to rescue the CycB + population of neuroblasts to the numbers seen in the thoracic hemisegments (Fig. 4D). As the *wor-GAL4* driver may not result in completely efficient inhibition of cell death, we performed the same experiment in two genetic backgrounds that completely lack neuroblast apoptosis: *grim*^{15E}*rpr*^{87}*/Df(3L)MM2* heterozygotes (referred to as *grim rpr/MM2*) and *Df(3L)H99* homozygous embryos (referred to as *H99/H99*). We again quantified the number of CycB+ (G2Q) and CycB- (G0) neuroblasts at embryonic stage 17 in these backgrounds. We observed that the number of abdominal G0 neuroblasts was equal to the number of G0 neuroblasts

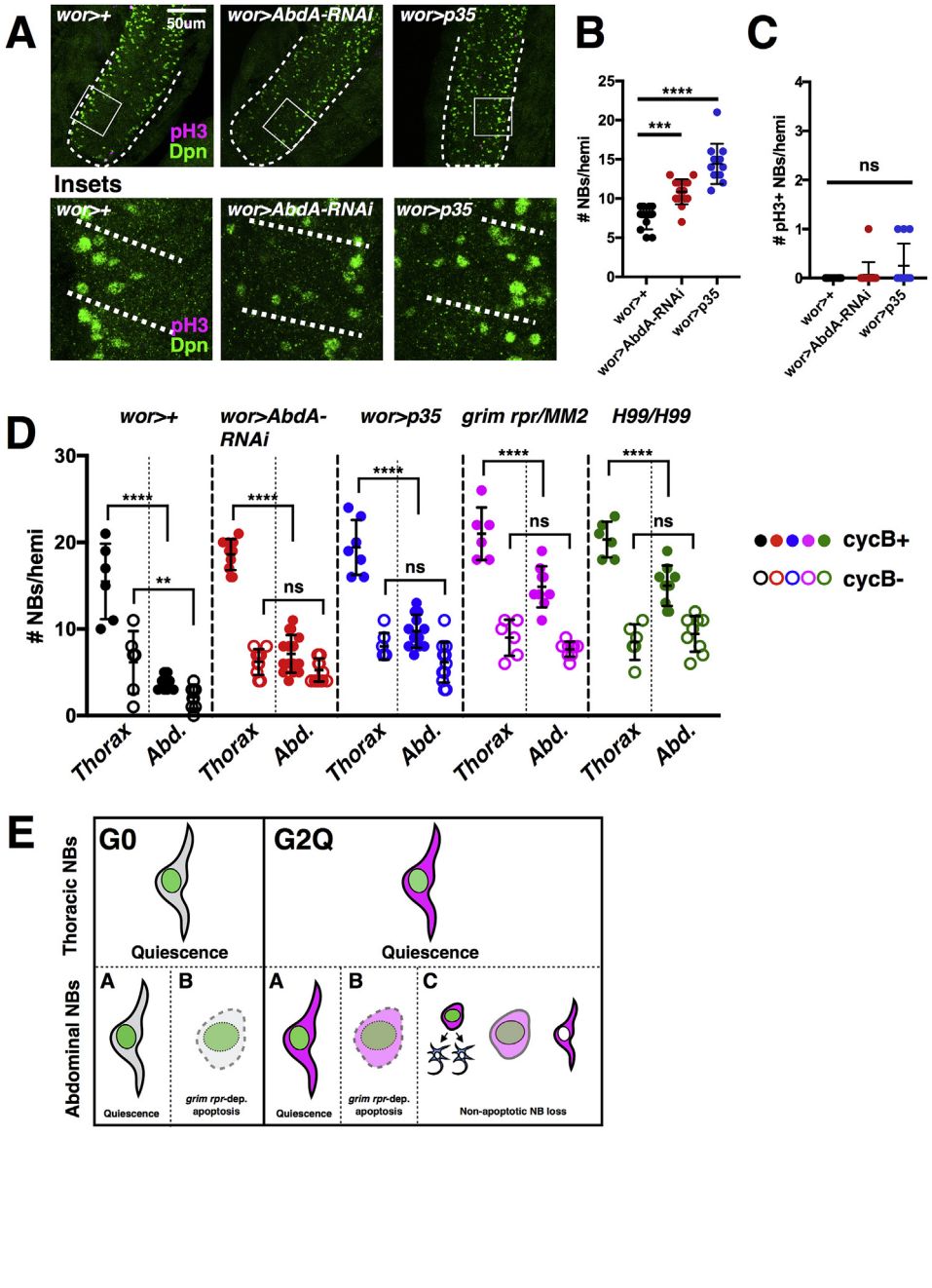

Fig. 4. Ectopic abdominal neuroblasts enter post-embryonic quiescence. (A–C) Abdominal neuroblasts, as detected by Dpn staining, that are rescued from cell death by knockdown of *abdA* or over-expression of the baculoviral broad-spectrum caspase inhibitor p35 cease proliferating at stage 17 of embryogenesis. The abdominal regions of the nervous system are outlined in white dotted lines. *abdA-RNAi* and *UAS-p35* both significantly increase the number of abdominal neuroblasts remaining at stage 17 **(B)**, but the vast majority of these neuroblasts are pH3-negative similar to control neuroblasts **(C)** (total $n > 4$ embryos, 3 hemisegments each). **(D)** The number of CycB-positive and CycB-negative neuroblasts in thoracic and abdominal hemisegments was compared in wild type embryos to embryos where cell death was inhibited. Cell death inhibition by *abdA-RNAi* and *UAS-p35,* or in the *grim rpr/MM2* and *H99/H99* backgrounds, which completely lack embryonic apoptosis, significantly rescues the CycB-negative (G0) population of abdominal neuroblasts, to a level comparable to the number of CycB-negative (G0) neuroblasts present in thoracic region. However, none of the genotypes results in a complete rescue of the presumptive CycB-positive G2Q population of neuroblasts to levels similar to the thoracic hemisegments. This suggests that this specific population of cells may be lost through a non-apoptotic mechanism. **(E)** Model describing neuroblast cell fates in the thoracic and abdominal regions of the nervous system during embryogenesis. Thoracic neuroblasts display both G0 and G2Q arrests, with G0 representing ~25% of the population and G2Q observed in the remaining ~75% of neuroblasts. Within the G0-fated neuroblast population, the corresponding abdominal neuroblasts either enter G0 at embryonic stage 17, or are eliminated by apoptosis, as this entire population is rescued in the absence of *grim* and *rpr* expression. The majority of thoracic neuroblasts belong to the G2Q category and arrest in a CycB-positive state at stage 17. Some, but not all, of the corresponding abdominal neuroblasts of the G2Q type are rescued in the absence of apoptosis. This finding suggests that the remaining abdominal neuroblasts within this population are eliminated from the embryo by a non-apoptotic mechanism that could include terminal division, non-apoptotic death such as autophagy, or loss of neuroblast identity as monitored by Dpn expression.

observed in thoracic hemisegments (Fig. 4D). However, we consistently found fewer G2Q neuroblasts than expected in the abdominal hemisegments in both *grim rpr/MM2* and *H99/H99* backgrounds, compared to the number observed in the thoracic hemisegments (Fig. 4D). There is no difference in the number of neuroblasts per hemisegment between the thorax and abdomen in *grim rpr/MM2* embryos at stage 14 (Fig. S5), indicating that the discrepancy in neuroblast number at the end of embryogenesis is not due to differences in neuroblast specification.

As the *grim rpr/MM2* and *H99/H99* mutant embryos lack all neuroblast apoptosis (White et al., 1994; Tan et al., 2011), we conclude that this subpopulation of G2Q-fated abdominal neuroblasts must be lost through a yet unknown non-apoptotic mechanism (Fig. 4E). Potential mechanisms for this observed G2Q-fated neuroblast loss could include a terminal division of the neuroblast, down-regulation of the Dpn protein used as a marker in this study, or a non-apoptotic cell death such as autophagy. We believe that this is the first demonstration of neuroblast loss in the embryonic nervous system in the absence of apoptosis.

3. Conclusions

In this study, we show that the neuroblast cell fate decisions of proliferation and cell death are decoupled during *Drosophila* embryogenesis. Our data indicate that developmental apoptosis occurs in a cell cycle-independent manner, which suggests that the activity of *Drosophila* cell death effectors is not subject to cell cycle-dependent regulation, as has been proposed in other systems (reviewed in Haschka et al., 2018). We conclude that, while factors such as *abdA* have been shown to regulate both neuroblast proliferation and cell death, these effects are independent of each other and represent distinct cell fate pathways.

In addition, we have shown that surviving neuroblasts can enter G2Q or G0 at the end of embryogenesis, indicating that the survival fate is not exclusive to either of these quiescence types. Neuroblast entry into

quiescence at the end of embryogenesis is dependent on the pseudokinase *tribbles* (Otsuki and Brand, 2018) and is associated with nuclear accumulation of the transcription factor *prospero* (Lai and Doe, 2014), but the upstream mechanisms that lead to the pause in neuroblast proliferation remain unclear. Our results indicate that entry into quiescence is not a cell-intrinsic property specific to neuroblasts that survive until the end of embryogenesis, and that ectopic neuroblasts remain competent to respond to the upstream signals that promote neuroblast quiescence. Finally, in examining the spatial patterns of quiescence in the abdominal region, we observed that a subset of abdominal neuroblasts are lost even in genetic backgrounds completely lacking neuroblast apoptosis. This proposed non-apoptotic neuroblast loss is specific to the abdominal neuroblasts that correspond to the G2Q-arrested neuroblasts in the thorax, indicating a potential shared point of regulation between these cell fate decisions. The connection between quiescence type and cell fate remains to be determined, but these findings have unveiled a new layer of neuroblast identity that will deepen our understanding of the pathways dictating stem cell behaviors.

4. Materials and methods

4.1. Fly stocks and genotypes

All flies were raised at 25 °C on cornmeal/yeast agar medium supplemented with live yeast. Cell cycle arrest experiments were performed at 29 °C, and *abdA-RNAi/UAS-p35* experiments were performed at 25 °C. The following stocks were used in this study: from Bloomington Stock Center, *UAS-NLS-dsRed/CyO* (#8546), *VAcht-GAL4* (#39220), *calx-GAL4/TM3* (#48160), *abdA-RNAi* (#35644), *cycE-RNAi* (#38902) and *cycA-RNAi* (#35694). *wor-GAL4* (Albertson et al., 2004) was previously recombined with *UAS-NLS-dsRed* to visualize driver expression (Arya et al., 2015). *UAS-p35* was generated by Hay et al. (1994). The *UAS--dap(2B)* stock was a kind gift from I. K. Hariharan. $grim^{15E}$ rpr^{87}*/TM3, GFP, Df(3L)MM2/TM3,GFP* and *Df(3L)H99* stocks have been described previously (Tan et al., 2011; White et al., 1994).

4.2. Embryo immunostaining

Primary antibodies used in this study: rat anti-Deadpan (1:150; Abcam ab195173), rabbit anti-pH3 (1:1000; Millipore 06–570), mouse anti-cycB (1:3; DSHB F2F4-s), rabbit anti-cDcp1 (1:100; Cell Signaling #9578), and rabbit anti-GFP (1:500; Thermo A11122). All secondary antibodies were used at 1:200 dilution in 1% nonfat milk (Molecular Probes). Embryos were blocked with 1% nonfat milk at least 30 min prior to the addition of primary antibodies. Primary incubations were performed for 2–3 days at 4 °C, and secondary incubations were performed for 2 h at room temperature or overnight at 4 °C. Embryos were mounted with Fluoromount G mounting medium (ThermoFisher, 00-4958-02).

4.3. Imaging, quantification and statistical analysis

All imaging was performed with a Nikon A1 confocal microscope at a z-resolution of 1.0 μm. All slides for a given experiment were imaged at the same confocal settings, and images were visualized and processed with FIJI at the same settings. Images are full maximal projections unless otherwise noted. Quantifications were performed on three abdominal hemisegments per embryo, as defined by the segmented pattern of the *wor* > *dsRed* driver. Progeny of NB3-5 were visualized by dsRed expression and defined as dsRed + nuclei in physical contact with adjacent cells in the cluster. Surviving neuroblasts were identified *in vivo* by their co-expression of dsRed and Dpn, and their anatomical position within the hemisegment. Expression of nuclear cycB was quantified as mean intensity within the nuclear area defined by Dpn expression and normalized by subtracting background mean intensity of five nearby areas of similar size within the same z-stack.

Graphs display mean values and standard deviation; *n* values are noted in figure legends. Statistical analyses were performed with Graphpad Prism: p-values were calculated with Dunnett's multiple comparisons test to accommodate multiple genotypes, or two-tailed Student's t-test (unequal variance) where applicable. The following convention was used for Dunnett's statistical significance with adjusted p-value: $p < 0.0332$(*), $p < 0.0021$(**), $p < 0.0002$(***), $p < 0.0001$(****).

Acknowledgements:

The authors thank Seda Gyonjyan and Katerina Heath for technical assistance and members of the Dyson lab for helpful comments on this project, as well as the Bloomington Drosophila Stock Center and Dr. Iswar Hariharan for fly lines, and the Developmental Studies Hybridoma Bank for antibodies. This research was supported by the National Institutes of Health R01GM110477 and R03NS092063, and an MGH Department of Dermatology seed grant to KW.

Appendix A. Supplementary data

Supplementary data to this article can be found online at https://doi.org/10.1016/j.ydbio.2019.08.004.

Conflicts of interest

The authors declare no competing interests.

References

Abrams, J.M., et al., 1993. Programmed Cell Death during Drosophila Embryogenesis. Development, pp. 29–43, 117.
Albertson, R., et al., 2004. Scribble protein domain mapping reveals a multistep localization mechanism and domains necessary for establishing cortical polarity. J. Cell Sci. 117 (Pt 25), 6061–6070.
Arya, R., et al., 2015. Neural stem cell progeny regulate stem cell death in a Notch and Hox dependent manner. Cell Death Differ. 22 (8), 1378–1387.
Bello, B.C., Hirth, F., Gould, A.P., 2003. A pulse of the Drosophila Hox protein abdominal-A schedules the end of neural proliferation via neuroblast apoptosis. Neuron (37), 209–219.
Birkholz, O., et al., 2015. Bridging the gap between postembryonic cell lineages and identified embryonic neuroblasts in the ventral nerve cord of Drosophila melanogaster. Biology Open 4, 420–434.
Britton, J.S., Edgar, B.A., 1998. Environmental control of the cell cycle in Drosophila: nutrition activates mitotic and endoreplicative cells by distinct mechanisms. Development 125 (11), 2149–2158.
Chao, H.X., et al., 2017. Orchestration of DNA damage checkpoint dynamics across the human cell cycle. Cell. Syst. 5 (5), 445–459 e5.
Chell, J.M., Brand, A.H., 2010. Nutrition-responsive glia control exit of neural stem cells from quiescence. Cell 143 (7), 1161–1173.
Chen, P., et al., 1996. grim, a novel cell death gene in Drosophila. Genes Dev. (10), 1773–1782.
Cosolo, A., et al., 2019. JNK-dependent Cell Cycle Stalling in G2 Promotes Survival and Senescence-like Phenotypes in Tissue Stress. eLife, pp. 1–65.
de Nooij, J.C., Letendre, M.A., Hariharan, I.K., 1996. A cyclin-dependent kinase inhibitor, dacapo, is necessary for timely exit from the cell cycle during Drosophila embryogenesis. Cell 87 (7), 1237–1247.
Ebens, A.J., et al., 1993. The Drosophila anachronism locus: a glycoprotein secreted by glia inhibits neuroblast proliferation. Cell 74, 15–27.
Fan, Y., et al., 2010. Dual roles of Drosophila p53 in cell death and cell differentiation. Cell Death Differ. 17 (6), 912–921.
Haschka, M., et al., 2018. Perturbing mitosis for anti-cancer therapy: is cell death the only answer? EMBO Rep. 19 (3) e45440–20.
Hassel, C., et al., 2013. Induction of endocycles represses apoptosis independently of differentiation and predisposes cells to genome instability. Development 141 (1), 112–123.
Hay, B.A., Guo, M., 2006. Caspase-dependent cell death in Drosophila. Annu. Rev. Cell Dev. Biol. 22 (1), 623–650.
Hay, B.A., Wolff, T., Rubin, G.M., 1994. Expression of Baculovirus P35 Prevents Cell Death in Drosophila. Development, pp. 2121–2129, 120.
Ito, K., Hotta, Y., 1992. Proliferation pattern of postembryonic neuroblasts in the brain of Drosophila melanogaster. Dev. Biol. 149 (1), 134–148.
Khandelwal, R., et al., 2017. Combinatorial action of grainyhead, extradenticle and notch in regulating Hox mediated apoptosis. In: Wang, H. (Ed.), PLoS Genetics Drosophila Larval CNS, vol. 13, e1007043, 10.
Lacin, H., Truman, J.W., 2016. Lineage mapping identifies molecular and architectural similarities between the larval and adult Drosophila central nervous system. eLife (5), 1–28.

Lai, S.-L., Doe, C.Q., 2014. Transient nuclear Prospero induces neural progenitor quiescence. eLife 3, 379–12.
Lane, M.E., et al., 1996. Dacapo, a cyclin-dependent kinase inhibitor, stops cell proliferation during Drosophila development. Cell 87 (7), 1225–1235.
Otsuki, L., Brand, A.H., 2018. Cell cycle heterogeneity directs the timing of neural stem cell activation from quiescence. Science 360 (6384), 99–102.
Pawlik, T.M., Keyomarsi, K., 2004. Role of cell cycle in mediating sensitivity to radiotherapy. Int. J. Radiat. Oncol. Biol. Phys. 59 (4), 928–942.
Peterson, C., et al., 2002. Reaper Is Required for Neuroblast Apoptosis during Drosophila Development. Development, pp. 1467–1476, 129.
Pfeiffer, B.D., et al., 2010. Refinement of tools for targeted gene expression in Drosophila. Genetics 186 (2), 735–755.
Qi, S., Calvi, B.R., 2016. Different cell cycle modifications repress apoptosis at different steps independent of developmental signaling in Drosophila. Mol. Biol. Cell (27), 1885–1897.
Ryl, T., et al., 2017. Cell-cycle position of single MYC-driven cancer cells dictates their susceptibility to a chemotherapeutic drug. Cell. Syst. 5 (3), 237–250 e8.
Song, Z., McCall, K., Steller, H., 1997. DCP-1, a Drosophila cell death protease essential for development. Science 275 (5299), 536–540.
Sousa-Nunes, R., Yee, L.L., Gould, A.P., 2011. Fat cells reactivate quiescent neuroblasts via TOR and glial insulin relays in Drosophila. Nature 471 (7339), 508–512.
Srinivasula, S.M., et al., 2002. Sickle, a novel Drosophila death gene in the reaper/hid/grim region, encodes an IAP-inhibitory protein. Curr. Biol. (12), 125–130.
Tan, Y., et al., 2011. Coordinated expression of cell death genes regulates neuroblast apoptosis. Development 138 (11), 2197–2206.
Truman, J.W., Bate, M., 1988. Spatial and temporal patterns of neurogenesis in the central nervous system of Drosophila melanogaster. Dev. Biol. (125), 145–157.
Tsuji, T., Hasegawa, E., Isshiki, T., 2008. Neuroblast entry into quiescence is regulated intrinsically by the combined action of spatial Hox proteins and temporal identity factors. Development 135 (23), 3859–3869.
White, K., et al., 1994. Genetic control of programmed cell death in Drosophila. Science 264, 677–683.
Wing, J.P., et al., 2002. Drosophila sickle is a novel grim-reaper cell death activator. Curr. Biol. (12), 131–135.